Comparison between Polymorphic Behaviors of Ziegler−Natta and Metallocene-Made Isotactic Polypropylene: The Role of the Distribution of Defects in the Polymer Chains

Claudio De Rosa,* Finizia Auriemma, Clementina Spera, Giovanni Talarico, and Oreste Tarallo

Dipartimento di Chimica, Università degli studi di Napoli "Federico II", Complesso Monte S. Angelo, Via Cintia, 80126 Napoli, Italy

Received September 3, 2003; Revised Manuscript Received December 3, 2003

ABSTRACT: A comparative analysis of the polymorphic behavior of samples of isotactic polypropylene (iPP) prepared with heterogeneous Ziegler−Natta catalysts and with a single-center homogeneous metallocene catalyst is presented. Different samples of Ziegler−Natta iPP, prepared with $MgCl_2$-supported catalysts modified by adding different Lewis bases, have been fractionated by extraction with boiling solvents. The irregular fraction, insoluble in diethyl ether and soluble in hexane, crystallizes from the melt almost totally in the γ form. The more stereoregular fractions crystallize instead basically in the α form. This confirms that, even in the case of Ziegler−Natta iPP samples, the γ form may develop by melt-crystallization at atmospheric pressure in fractions containing a high concentration of defects. The relative amount of γ form crystallized from the melt is, however, much lower that that observed in samples of metallocene-made iPP containing comparable amount of defects. Since the γ form crystallizes in chains having short regular isotactic sequences, these data indicate that in Ziegler−Natta iPP samples the regular isotactic sequences are longer than those present in chains of metallocene-made iPP having a similar overall concentration of defects. The different polymorphic behavior of metallocene and Ziegler−Natta iPP samples is related to the different distribution of defects in the polymeric chains, generated by the different kinds of catalytic systems. While in the metallocene-made iPP the distribution of defects along the chains is random, in Ziegler−Natta iPP samples the majority of the defects are segregated in a small fraction of poorly crystallizable macromolecules or in more irregular portions of the chain, so that much longer fully isotactic sequences can be produced, leading to the crystallization of the α form, even for a relatively high overall concentration of defects. These results confirm the idea that the structural analysis of iPP, in particular the crystallization of the γ form, may give information about the microstructure of the polymer chains. The measure of the maximum amount of γ form crystallized from the melt may be used as an indirect method to evaluate the average length of isotactic sequences. This analysis allows concluding that some fractions of Ziegler−Natta iPP are characterized by chains with a stereoblock microstructure, consisting of regular isotactic sequences linked to more irregular sequences. The latter contain the major part of stereodefects mainly consisting in isolated *rr* triads, *r* diads, and longer ...*rrrr*... syndiotatic sequences. The hypothesis of a stereoblock microstructure for some of these less stereoirregular fractions is also consistent with the high degree of crystallinity observed in the samples crystallized from solution or from the melt, despite the high concentration of defects.

Introduction

Isotactic polypropylene (iPP) presents a complex polymorphic behavior.[1,2] Three different crystalline forms (α, β, and γ forms)[1−8] and a mesomorphic form[9] have been described. All the polymorphic forms are characterized by chains in the stable 3-fold helical conformation.[1] The polymorphic behavior is complicated by the presence of structural disorder in the crystalline forms.[10−14]

Commercial iPP, prepared with the traditional heterogeneous Ziegler−Natta catalytic systems, generally crystallizes in the stable α form.[1,2] The β and γ forms may be obtained only under special conditions of crystallization. The β form, indeed, crystallizes only in the presence of nucleating agents,[2,5,6] whereas the γ form can be obtained only by crystallization from the melt at elevated pressures (about 5000 atm)[15] or by crystallization at atmospheric pressure of low molecular weight samples[16] and of copolymers containing small amounts (in the range 5−20 mol %) of other olefins.[17]

With the development of metallocene catalytic systems for the isospecific polymerization of olefins, new isotactic polypropylenes, showing a wide variety of microstructures, have become available.[18] Depending on the specific metallocene catalyst, as well as on the polymerization conditions (i.e., monomer concentration, temperature, nature of cocatalyst, etc.), iPP samples containing different amounts and combinations of defects of stereoregularity (primary insertions with the wrong enantioface, or stereodefects) and regioregularity (meso and racemo secondary insertions, or regiodefects) can be obtained.[18]

The polymorphic behavior of metallocene-made iPP samples, and, in particular, the relative stability of the α and γ forms under common conditions of crystallization, is completely different from that of iPP samples prepared with heterogeneous catalysts and is closely related to their microstructure.[19−27]

iPP samples prepared with homogeneous metallocene catalysts crystallize more easily in the γ form, even at atmospheric pressure and for high molecular weight samples.[19−27] The different polymorphic behavior of iPP samples prepared with heterogeneous and homogeneous

* Corresponding author: Telephone ++39 081 674346; Fax ++39 081 674090; e-mail derosa@chemistry.unina.it.

10.1021/ma035295q CCC: $27.50
Published on Web 01/21/2004

catalysts is related to the different type and distribution along the chains of insertion mistakes, that is, stereodefects and regiodefects, generated by the different kinds of catalytic systems. The distribution of defects, in turn, influences the average length of the crystallizable (fully isotactic) sequences.

In recent papers it has been clearly shown that when the fully isotactic sequences are very short, iPP crystallizes in the γ form, whereas very long regular isotactic sequences generally crystallize only in the α form.[19,25−27] In chains of iPP samples prepared with *ansa*-metallocene catalysts the distribution of defects is random, and the length of fully isotactic sequences is roughly inversely related to the content of insertion errors.[25,26] As a consequence, even a small amount of defects reduces the length of the regular isotactic sequences inducing the crystallization of the γ form.[19,25,26] In the case of iPP samples obtained with heterogeneous Ziegler−Natta catalytic systems, instead, the majority of the defects may be segregated in a small fraction of poorly crystallizable macromolecules, so that much longer, fully isotactic sequences can be produced, leading to the crystallization of the α form even for a relatively high overall concentration of defects.

The crystallization properties of metallocene-made iPP have been analyzed in samples characterized by chains including different types of microstructural defects (strereodefects and regiodefects).[19−27] Mixtures of the α and γ forms are generally obtained by isothermal crystallization from the melt, and the content of γ form increases with increasing the content of defects.[19,22,23,25−27] The formation of the γ form seems to be favored by the presence of stereodefects (mainly *rr* isolated triads),[19,25−27] and/or regiodefects (mainly 2,1 and 3,1 insertions),[19,22] and also by the presence of constitutional defects, like comonomeric units.[21,23]

In a recent paper,[26] we have analyzed the polymorphic behavior of metallocene iPP samples characterized by a very simple microstructure, containing only defects of stereoregularity (only isolated *rr* triads),[28] providing the first example of structural study on metallocene-made iPP not including regioerrors. This allowed us to suggest a more unified view of the crystallization of metallocene iPP.[26] Samples of iPP prepared with metallocene catalysts crystallize from the melt in mixtures of crystals of α and γ forms. The content of γ form increases with increasing the concentration of defects, due to the reduced length of the regular isotactic sequences,[26] and increasing the crystallization temperature. Crystals of the γ form obtained in these samples always present structural disorder,[26] characterized by defects in the regular packing of bilayers of chains with axes oriented alternatively along two nearly perpendicular directions.[24−26] This disorder produces a local situation of packing typical of the α form, with some adjacent bilayers having parallel chains (α/γ disorder). Therefore, metallocene iPP crystallizes in a continuum of disordered modifications intermediate between α and γ forms, the amount of disorder being dependent on the crystallization conditions and on the stereoregularity of the sample.

The increase of the content of γ form with increasing the crystallization temperature has been explained as a result of two competing kinetic and thermodynamic effects.[26] For samples of iPP, containing an appreciable amount of stereodefects, the formation of the γ form is thermodynamically favored, since either the *rr* defects or the α/γ structural disorder are highly tolerated in the γ form. As a consequence, a high amount of γ form develops in the slow crystallizations at high temperatures. At lower crystallization temperatures the fast crystallization of the α form is instead kinetically favored, giving a low amount of γ form. With increasing the crystallization temperature the amount of γ form increases, but at very high crystallization temperatures (higher than 130 °C) the crystallization of the defective γ form is too slow because of its lower melting temperature, and the more perfect α form becomes again kinetically favored, so that the amount of γ form decreases.[26]

We have recently shown for the first time that also the kind of distribution of defects along the polymer chains influences the polymorphic behavior of iPP and the crystallization of the γ form.[25] We have, indeed, demonstrated that in the case of stereoblock polypropylene, prepared with oscillating metallocene catalysts,[29] the amount of γ form which develops in the melt-crystallization procedures is much lower than that obtained for iPP samples having the same overall concentration of defects, but prepared with stereorigid metallocene catalysts, which produce a random distribution of defects.[25] This has been explained considering that in the stereoblock polypropylene most of the defects are segregated in stereoirregular, noncrystallizable blocks, which alternate to more regular isotactic sequences, long enough to crystallize in the α form.[25] This result confirms that the γ form crystallizes when the fully isotactic sequences are very short.[25,26] Our studies have, therefore, demonstrated that it is possible to obtain information about the microstructure of iPP chains (distribution of defects and inclusion of defects in the crystals) through the indirect method of the structural analysis.[25]

Once the role of the stereodefects and the distribution of defects along the polymer chains on the polymorphic behavior of iPP has been clarified, the method of the structural analysis may be extended to iPP samples having a more complex microstructure, as commercial iPP produced with the multisited heterogeneous Ziegler−Natta catalysts. The different types of catalyst sites present on the surfaces of the heterogeneous Ziegler−Natta catalyst lead to mixtures of polypropylene molecules having different molecular weights, different stereoregularities, and distributions of stereosequences. Ziegler−Natta iPP samples can be generally fractionated with conventional methods of extraction with boiling solvents in different fractions characterized by different microstructures, which reflect the different crystallinities and melting behavior. The microstructures of fractions of Ziegler−Natta iPP have been studied by ^{13}C NMR spectroscopy,[30−38] clearly indicating a nonuniform interchain composition of defects. The majority of the defects are segregated in a small fraction of poorly crystallizable macromolecules or in small portions (more irregular blocks) of long regular chains, producing in any case long regular isotactic sequences. For this reason, even a nonnegligible amount of defects does not greatly influence the crystallization properties of iPP. In fact, the regular isotactic sequences are long enough to crystallize in the α form with melting temperatures generally higher than those observed in metallocene iPP. When the defects are randomly distributed along the polymer chains, as in metallocene-made iPP, the regular isotactic sequences are short,

Table 1. Results of the Fractionation of the Sample T1: Weight Fractions (%), Intrinsic Viscosities ([η]), Molecular Masses (M_v), Melting Temperatures (T_m), Melting Enthalpies (ΔH_m), and Crystallinity Indices (x_c) of the Sample T1 and of the Corresponding Four Fractions

fractions	wt %	[η] (dL/g)	M_v[a]	T_m (°C)[b]	ΔH_m (J/g)	x_c[c]
T1(EtS)	23	0.48	3.88×10^4			0.07[d]
T1(EtI−HsS)	7	0.56	4.76×10^4	114	36.2	0.17
T1(HsI−HS)	10	0.67	5.98×10^4	148	70.0	0.33
T1(HI)	60	1.51	1.81×10^5	146, 160	110.4	0.53
whole sample T1	100	1.42	1.66×10^5	159	57.0	0.27

[a] From the intrinsic viscosities using the parameters of the Mark−Houwink equation $\alpha = 0.74$ and $k = 1.93 \times 10^{-4}$ dL/g.[41b] [b] Peak temperatures from the DSC curves recorded at heating rate of 10 °C/min (Figure 4). [c] From the melting enthalpies ΔH_m, $x_c = \Delta H_m/\Delta H_m°$ assuming as thermodynamic melting enthalpy $\Delta H_m° = 209.5$ J/g.[42] [d] From the X-ray powder diffraction profile of Figure 3a, in the corresponding DSC curve no signal was detected.

Table 2. Results of the Fractionation of the Sample T2: Weight Fractions (%), Intrinsic Viscosities ([η]), Molecular Masses (M_v), Melting Temperatures (T_m), Melting Enthalpies (ΔH_m), and Crystallinity Indices (x_c) of the Sample T2 and of the Corresponding Three Fractions

fractions	wt %	[η] (dL/g)	M_v[a]	T_m (°C)[b]	ΔH_m (J/g)	x_c[c]
T2(AS)	0.9					
T2(AI−XS)	27.4	0.52	4.24×10^4			0.05[d]
T2(XI)	71.7	1.13	1.22×10^5	155	80.9	0.39
whole sample T2	100	1.02	1.07×10^5	160	39.4	0.19

[a] From the intrinsic viscosities using the parameters of the Mark−Houwink equation $\alpha = 0.74$ and $k = 1.93 \times 10^{-4}$ dL/g.[41b] [b] Peak temperatures from the DSC curves recorded at heating rate of 10 °C/min. [c] From the melting enthalpies ΔH_m, $x_c = \Delta H_m/\Delta H_m°$ assuming as thermodynamic melting enthalpy $\Delta H_m° = 209.5$ J/g.[42] [d] From the X-ray powder diffraction profile of Figure 5b, in the corresponding DSC curve no signal was detected.

even for a small amount of defects, producing crystallization of the γ form with lower melting temperatures.[19,22−26]

As recently pointed out by Alamo et al.,[39] since it is important to identify the possibility of a nonrandom intramolecular distribution or blocky stereosequences in iPP chains, other types of physical evidence must be utilized in conjunction with ^{13}C NMR. For this purpose, indirect methods must be used to identify the microstructure of the iPP molecule, as for instance the method of the structural analysis proposed by us in the ref 25. In that paper[25] we were able to deduce the blocky microstructure of the elastomeric polypropylene[29] from the analysis of its crystallization properties. Moreover, Alamo and Randall et al. have analyzed the crystallization behavior of metallocene and Ziegler−Natta iPP, providing evidence of the different intramolecular distribution of defects in each type of iPP from the analysis of the crystallization rates of the samples, associated with the ^{13}C NMR data.[39,40]

In this paper the crystallization properties and the polymorphic behavior of fractions of Ziegler−Natta iPP are analyzed and compared with the behavior of metallocene iPP. From the amount of γ form, which develops by crystallizations from the melt, information about the microstructures of the fractions in Ziegler−Natta iPP can be obtained.

Experimental Section

Two samples of Ziegler−Natta iPP (samples T1 and T2) were supplied by Basell Polyolefins (Ferrara, Italy). The sample T1 was prepared with a $MgCl_2$-supported Ziegler−Natta catalyst, modified using di(isobutyl) phthalate as internal donor. The sample T2 was prepared with a $MgCl_2$-supported Ziegler−Natta catalyst, modified using di(isobutyl) phthalate as internal donor and cyclohexylmethyldimethoxysilane as external donor. The molar ratio between triethylaluminum and external donor was 300 mol/mol. The two samples were fractionated by Kumagawa extraction with boiling solvents or by fractional crystallization after dissolution in *o*-xylene.

The sample T1 was fractionated by exhaustive Kumagawa extraction using sequentially boiling diethyl ether (Et), hexane (Hs), and heptane (H). Fractions soluble in diethyl ether (T1(EtS)), insoluble in diethyl ether and soluble in hexane (T1(EtI−HsS)), insoluble in hexane and soluble in heptane (T1(HsI−HS)), and, finally, insoluble in heptane (T1(HI)) were separated (Table 1). The sample T2 was fractionated by fractional crystallization from *o*-xylene solution. The sample was first dissolved in *o*-xylene at 135 °C. The homogeneous solution was slowly cooled to room temperature, allowing precipitation of the more stereoregular and crystalline fraction. The fraction insoluble in *o*-xylene (T2(XI)) was separated. The fraction soluble in *o*-xylene was further fractionated in acetone, and a more irregular fraction soluble in acetone (T2(AS)) was separated from the fraction insoluble in acetone and soluble in *o*-xylene (T2(AI−XS)) (Table 2). All fractions were characterized by solution viscosimetry,^{13}C NMR spectroscopy, differential scanning calorimetry (DSC), and X-ray diffraction (Tables 1 and 2).

Three samples of metallocene-made iPP (samples R1, R2, and R3) were provided by Dr. Luigi Resconi of Basell Polyolefins (Ferrara, Italy). They were synthesized at different temperatures using the single-center catalyst *rac*-isopropylidene[bis(3-trimethylsilylindenyl)]zirconium dichloride, activated with methylaluminoxane (MAO), as described in ref 28. As shown by Resconi et al.,[28] this catalyst produces iPP samples characterized by chains containing only defects of stereoregularity (mainly isolated *rr* triads), whose amount depends on the polymerization temperature. The distribution of defects along the chains is random, and no defects of regioregularity are present. The molecular weights, the melting temperatures, and the main microstructural characteristics of the three samples are reported in Table 3.

The intrinsic viscosities were measured in 1,2,3,4-tetrahydronaphthalene solutions at 135 °C, using standard Ubbelohde viscosimeter, with a single point technique.[41a] The molecular weights were evaluated from the intrinsic viscosities using the parameters reported for isotactic polypropylene.[41b]

The ^{13}C NMR spectra of the various fractions of the samples T1 and T2 were recorded on a Varian XL-200 operating at 50 MHz in the Fourier transform mode of 10% w/v polymer solutions in deuterated tetrachloroethane (also used as internal standard) at 70 °C (fractions T1(EtS), T1(EtI−HsS), and T2(AI−XS)) and at 125 °C (fractions T1(HsI−HS), T1(HI), and T2(XI)).

The calorimetric measurements were performed with a differential scanning calorimeter (DSC), Perkin-Elmer DSC-7, in a flowing N_2 atmosphere. The melting temperatures of

Table 3. Polymerization Temperatures (T_{pol}), Concentrations of the Isotactic Pentad [*mmmm*] and of the Meso Diad [*m*], Triads Distribution, Molecular Masses (M_w), Melting Temperatures (T_m), Melting Enthalpies (ΔH_m), and Crystallinity Indices (x_c) of the As-Prepared Powders of the Three Metallocene-Made iPP Samples Prepared with the Highly Regiospecific *rac*-Isopropyliden[bis(3-trimethylsilyl)(indenyl)]zirconium dichloride/MAO Catalytic System[28]

samples	T_{pol} (°C)	[*mmmm*] (%)	[*m*] (%)	[*mm*] (%)	[*mr*] (%)	[*rr*] (%)	M_w	T_m (°C)[a]	ΔH_m (J/g)	x_c[b]
R1	20	89.0	95.5	93.3	4.4	2.3	110 000	144	96.5	0.46
R2	50	87.4	94.8	92.1	5.2	2.6	75 000	141	87.0	0.41
R3	60	83.4	93.1	89.7	6.9	3.4	66 000	137	76.0	0.36

[a] Melting temperature measured from DSC scans of the "as prepared" samples recorded at heating rate of 10 °C/min. [b] From the melting enthalpies ΔH_m, $x_c = \Delta H_m/\Delta H_m°$ assuming as thermodynamic melting enthalpy $\Delta H_m° = 209.5$ J/g.[42]

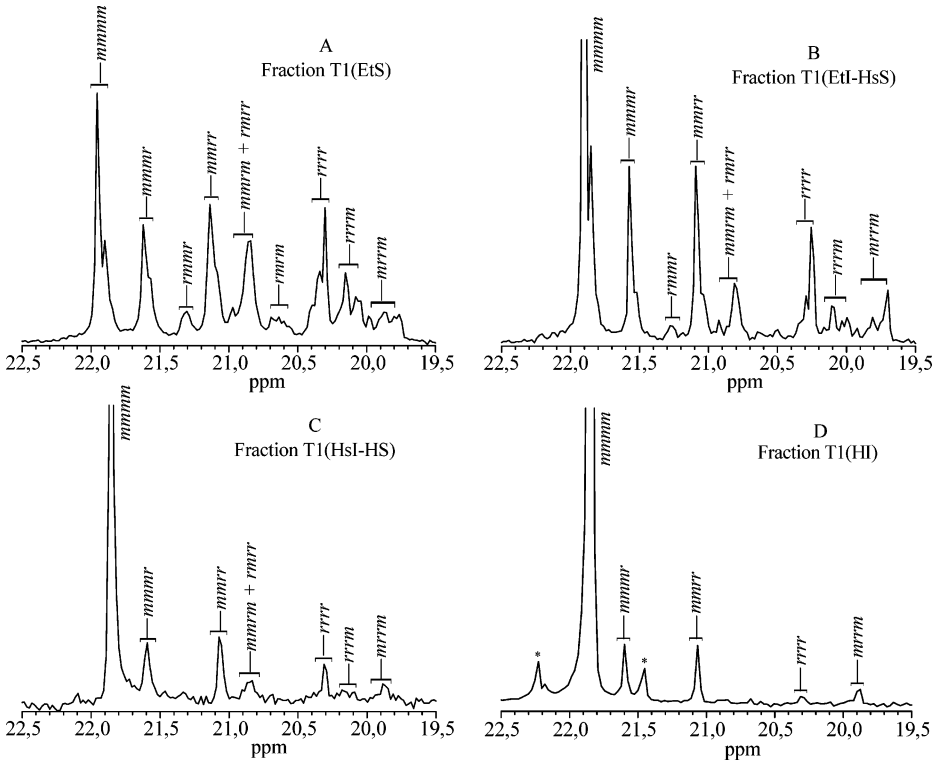

Figure 1. ^{13}C NMR spectra in the region of the methyl carbon atoms resonance of the fractions T1(EtS) (A), T1(EtI−HsS) (B), T1(HsI−HS) (C), and T1(HI) (D) of the iPP sample T1. The resonances indicated with asterisks in D correspond to the satellite peaks of the *mmmm* resonance.

the samples were taken as the peak temperature of the DSC curves.

The various fractions of the samples T1 and T2 were isothermally crystallized from the melt at different temperatures. Compression-molded specimens were melted at 180 or 200 °C and kept for 5 min at this temperature in a N_2 atmosphere; they were then rapidly cooled to the crystallization temperature, T_c, and kept at this temperature, still in a N_2 atmosphere, for a time t_c long enough to allow complete crystallization at T_c. The samples were then rapidly cooled to room temperature and analyzed by X-ray diffraction. In the various isothermal crystallizations, the crystallization time t_c is different depending on the crystallization temperature. The shortest time is 24 h for the lowest crystallization temperature and increases with increasing the crystallization temperature, up to 2 weeks for the highest crystallization temperature.

X-ray powder diffraction patterns were obtained at room temperature with an automatic Philips diffractometer using Ni-filtered Cu Kα radiation.

The relative amount of crystals in the γ form present in our samples was measured from the X-ray diffraction profiles, as suggested by Turner-Jones et al.,[43] by measuring the ratio between the intensities of the $(117)_\gamma$ reflection at $2\theta = 20.1°$, typical of the γ form, and the $(130)_\alpha$ reflection at $2\theta = 18.6°$, typical of the α form: $f_\gamma = I(117)_\gamma/[I(130)_\alpha + I(117)_\gamma]$. The intensities of $(117)_\gamma$ and $(130)_\alpha$ reflections were measured from the area of the corresponding diffraction peaks above the amorphous halo in the X-ray powder diffraction profiles. The amorphous halo has been obtained from the X-ray diffraction profile of an atactic polypropylene, and then it was scaled and subtracted to the X-ray diffraction profiles of the melt-crystallized samples.

Results and Discussion

As-Fractionated Samples. The Ziegler−Natta sample T1 has been fractionated with boiling diethyl ether, hexane, and heptane. The fractions soluble in diethyl ether (T1(EtS)), insoluble in diethyl ether and soluble in hexane (T1(EtI−HsS)), insoluble in hexane and soluble in heptane (T1(HsI−HS)) and, finally, insoluble in heptane (T1(HI)) have been separated. The weight fractions and the physical properties (melting temperature, intrinsic viscosity, molecular weight) of the four fractions are reported in Table 1. The ^{13}C NMR spectra in the region of the methyl carbon atom resonance of the four fractions are reported in Figure 1. The concentrations of the pentad stereosequences in the four fractions, evaluated from the ^{13}C NMR spectra of Figure 1, are shown in Table 4.

The sample T2 has been fractionated with *o*-xylene and acetone as described in the Experimental Section. The fraction soluble in *o*-xylene and insoluble in acetone (T2(AI-XS)) and the fraction insoluble in *o*-xylene (T2-(XI)) have been analyzed. The weight fractions and the

Table 4. Concentration of Pentad Stereosequences, from the ^{13}C NMR Spectra of Figure 1 in the Various Fractions of the Sample T1

fractions sample T1	[*mmmm*] (%)	[*mmmr*] (%)	[*rmmr*] (%)	[*mmrr*] (%)	[*mmrm*] + [*rmrr*] (%)	[*rmrm*] (%)	[*rrrr*] (%)	[*rrrm*] (%)	[*mrrm*] (%)
T1(EtS)	21.08	12.51	4.45	14.61	14.60[a]	4.28	12.45	9.75	6.28
T1(EtI−HsS)	47.54	11.42	1.76	12.80	6.82[b]		9.22	4.85	5.60
T1(HsI−HS)	74.68	6.64		7.27	2.94[c]		4.63	1.60	2.24
T1(HI)	91.44	3.68		3.07			0.63		1.18

[a] The resonance of low intensity at 20.96 ppm in the spectrum of Figure 1A corresponds to the *mmmrmr* sequence, whereas the resonance of higher intensity at 20.84 ppm corresponds mostly to the sequences *rrmrrm* and *rrmrrr*.[35] [b] The resonance of low intensity at 20.92 ppm in the spectrum of Figure 1B corresponds to the *mmmrmr* sequence, whereas the resonance of higher intensity at 20.81 ppm corresponds mostly to the sequences *rrmrrm* and *rrmrrr*.[35] [c] The broad resonance at 20.85 ppm in the spectrum of Figure 1C is due to the contributions of *mmmrmr*, *rrmrrm*, and *rrmrrr* sequences.

Table 5. Concentration of Pentad Stereosequences, from the ^{13}C NMR Spectra of Figure 2, in the Two Fractions of the Sample T2

fractions sample T2	[*mmmm*] (%)	[*mmmr*] (%)	[*rmmr*] (%)	[*mmrr*] (%)	[*mmrm*] + [*rmrr*] (%)	[*rmrm*] (%)	[*rrrr*] (%)	[*rrrm*] (%)	[*mrrm*] (%)
T2(AI−XS)	17.63	12.10	4.16	15.21	13.52[a]		16.96	11.59	8.87
T2(XI)	84.89	4.16	1.19	4.26	0.92		1.30	1.22	2.08

[a] The resonance of low intensity at 20.9 ppm in the spectrum of Figure 2A corresponds to the *mmmrmr* sequence, whereas the resonance of higher intensity at 20.78 ppm corresponds mostly to the sequences *rrmrrm* and *rrmrrr*.[35]

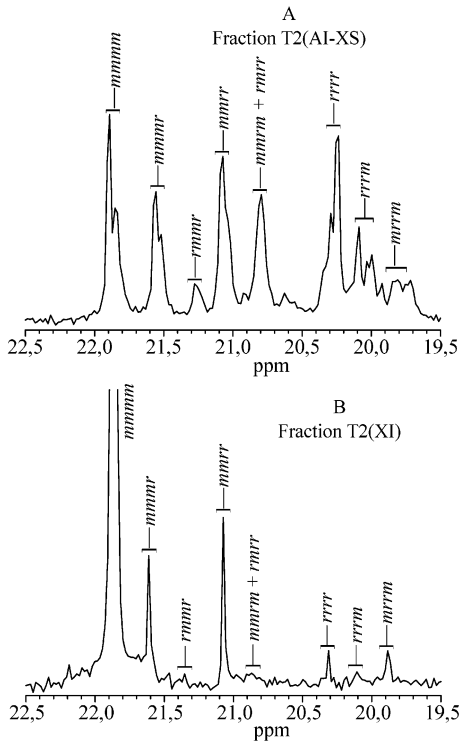

Figure 2. ^{13}C NMR spectra in the region of the methyl carbon atoms resonance of the fractions T2(AI-XS) (A) and T2(XI) (B) of the iPP sample T2.

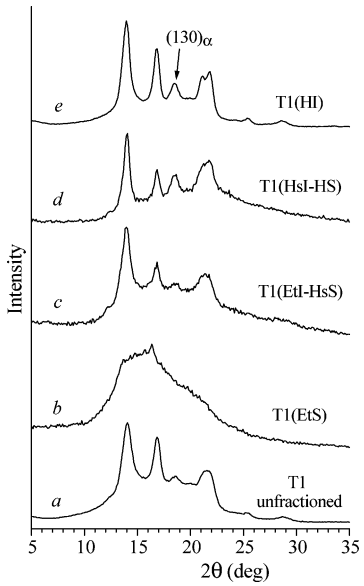

Figure 3. X-ray powder diffraction profiles of the as-prepared iPP sample T1 (a) and of the corresponding fractions T1(EtS) (b), T1(EtI−HsS) (c), T1(HsI−HS) (d), and T1(HI) (e). The $(130)_\alpha$ reflection of the α form at $2\theta = 18.6°$ is indicated.

physical properties (melting temperature, intrinsic viscosity, molecular weight) of the fractions are reported in Table 2. The ^{13}C NMR spectra in the region of the methyl carbon atom resonance of the two fractions are reported in Figure 2. The concentrations of the pentad stereosequences in the two fractions, evaluated from the ^{13}C NMR spectra of Figure 2, are shown in Table 5.

It is apparent that the fractions of the two Ziegler−Natta iPP samples show different distributions of pentads stereosequences, in particular a higher concentration of the fully syndiotactic *rrrr* pentad is present in the fractions of the sample T2 (Table 5). Even the more isotactic fraction T2(XI) presents a nonnegligible concentration of syndiotactic sequences ([*rrrr*] = 1.30%), which is instead very small in the fraction T1(HI) (0.6%, Table 4). It is well-known that different microstructures of chains in Ziegler−Natta iPP can be obtained depending on the catalyst, in particular on the Lewis bases added to the catalyst/cocatalyst system as internal or external donor.[35,36]

The X-ray powder diffraction profiles of the as-prepared sample T1 and of the four corresponding fractions are reported in Figure 3. The fraction soluble in diethyl ether (T1(EtS)) is basically amorphous (only a negligible crystallinity is observed in the profile b of Figure 3) due to the very low stereoregularity (Tables 1 and 4).

The other fractions, as well as the unfractionated sample, show a significant crystallinity, which increases for fractions insoluble in high boiling temperature solvents (Figure 3c−e). We recall that α and γ forms of iPP present similar X-ray diffraction profiles, the main difference being the position of the third strong diffraction peak, which occurs at $2\theta = 18.6°$ ($(130)_\alpha$ reflection) in the α form[1] and at $2\theta = 20.1°$ ($(117)_\gamma$ reflection) in

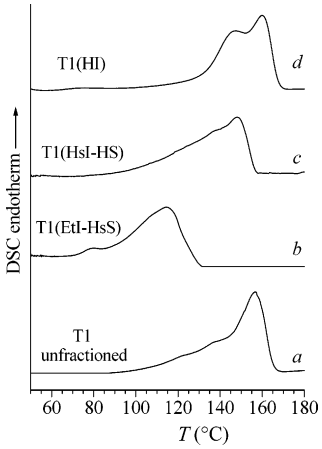

Figure 4. DSC curves, recorded at heating rate of 10 °C/min, of the as-prepared iPP sample T1 (a) and of the corresponding fractions T1(EtI−HsS) (b), T1(HsI−HS) (c), and T1(HI) (d).

the γ form.[7,8] It is apparent that the crystalline fractions, as well as the unfractionated sample, are mainly crystallized in the α form of iPP, as indicated by the presence of the $(130)_\alpha$ reflection at $2\theta = 18.6°$ of the α form and the absence of the $(117)_\gamma$ reflection at $2\theta = 20.1°$ of the γ form in the X-ray diffraction profiles of Figure 3a,c−e. The low intensity of the $(130)_\alpha$ reflection of the α form, with respect to that expected for crystals if the pure α form,[1] observed in the diffraction profiles of some fractions (Figure 3a,c,e), indicates that structural disorder (of the kind described in the refs 24 and 26) in the stacking of bilayers of 3-fold helical chains along the *b* axis is present in the crystals. According to the model of disorder proposed in refs 24 and 26, consecutive bilayers of chains may face each other with the chain axes either parallel (like in the α form) or nearly perpendicular (like in the γ form), producing disordered modifications intermediate between α and γ forms (α/γ disorder).[26] It is worth noting that the crystallization of iPP in α/γ disorder modifications, described for metallocene-made iPP samples,[24−26] is here recognized also for fractions of Ziegler−Natta iPP.

The DSC heating curves of the unfractionated T1 sample and of the corresponding fractions are reported in Figure 4. The melting temperatures and the crystallinities evaluated from the DSC curves are reported in Table 1. The broad DSC curve of the unfractionated sample (Figure 4a) is a result of the melting of the various fractions and shows peak melting temperature at 159 °C, due basically to the melting of the more crystalline fraction T1(HI) (Figure 4d), which is present in the sample T1 with highest concentration (60%, see Table 1).

The X-ray powder diffraction profiles of the as-prepared sample T2 and of the two corresponding fractions are reported in Figure 5. It is apparent that the fraction soluble in xylene T2(AI−XS) is basically amorphous; only a very small crystallinity is, indeed, observed in the profile b of Figure 5. Only a weak diffraction peak at $2\theta = 17°$, corresponding to the $(040)_\alpha$ reflection of the α form or the $(008)_\gamma$ reflection of the γ form of iPP, is present in the diffraction profile of Figure 5b. The absence of the other reflections of α and γ forms of iPP indicates that, as demonstrated in ref 24, the small crystals of iPP present in the fraction T2(AI−XS) are characterized by disordered modifications intermediate between α and γ forms containing the α/γ disorder described in refs 24 and 26 and discussed above. In the

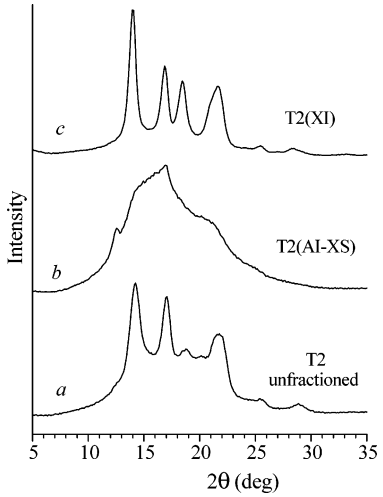

Figure 5. X-ray powder diffraction profiles of the as-prepared iPP sample T2 (a) and of the corresponding fractions T2(AI−XS) (b) and T2(XI) (c).

diffraction profile of Figure 5b also a weak diffraction peak at $2\theta = 12°$ is apparent. This peak arises from the diffraction of crystals of syndiotactic polypropylene[44] and indicates that in this sample the syndiotactic sequences are long enough to crystallize. The unfractionated T2 sample and the more crystalline fraction T2(XI) are basically crystallized in the α form (Figure 5a,c).

Melt-Crystallized Samples. The crystalline fractions of the samples T1 and T2 have been isothermally crystallized from the melt at different temperatures and analyzed by X-ray diffraction. The X-ray powder diffraction profiles of samples of the three fractions T1(EtI−HsS), T1(HsI−HS), and T1(HI) isothermally crystallized from the melt are reported in Figure 6. The diffraction profiles of the as-fractionated samples (already shown in Figure 3) are also reported in Figure 6 (profiles a) for comparison. It is apparent that, whereas the as-fractionated samples are basically in the α form (profiles a of Figure 6), the diffraction profiles of samples crystallized from the melt of Figure 6 always present the $(117)_\gamma$ reflection at $2\theta = 20.1°$ of the γ form, indicating that for all the iPP fractions crystals of the γ form develop when the samples are crystallized from the melt (profiles b−e of Figure 6A,B and profiles b−f of Figure 6C).

In particular, the fraction T1(EtI−HsS), initially in the α form with low crystallinity (profile a of Figure 6A), crystallizes from the melt almost totally in the γ form, although with low crystallinty, as indicated by the high intensity of the $(117)_\gamma$ reflection of the γ form at $2\theta = 20.1°$ at any crystallization temperature and the very low intensity of the $(130)_\alpha$ reflection of the α form at $2\theta = 18.6°$ in the diffraction profiles b−e of Figure 6A.

The other two more stereoregular fractions T1(HsI−HS) and T1(HI) crystallize from the melt in mixtures of crystals of α and γ forms, with higher amounts of the α form at any crystallization temperature, as indicated by the high intensity of the $(130)_\alpha$ reflection of the α form at $2\theta = 18.6°$ and the low intensity of the $(117)_\gamma$ reflection at $2\theta = 20.1°$ in the diffraction profiles of Figure 6B,C. For these samples the crystallinity is much higher than that developed for the fraction T1(EtI−HsS).

The X-ray powder diffraction profiles of samples of the fraction T2(XI), isothermally crystallized from the

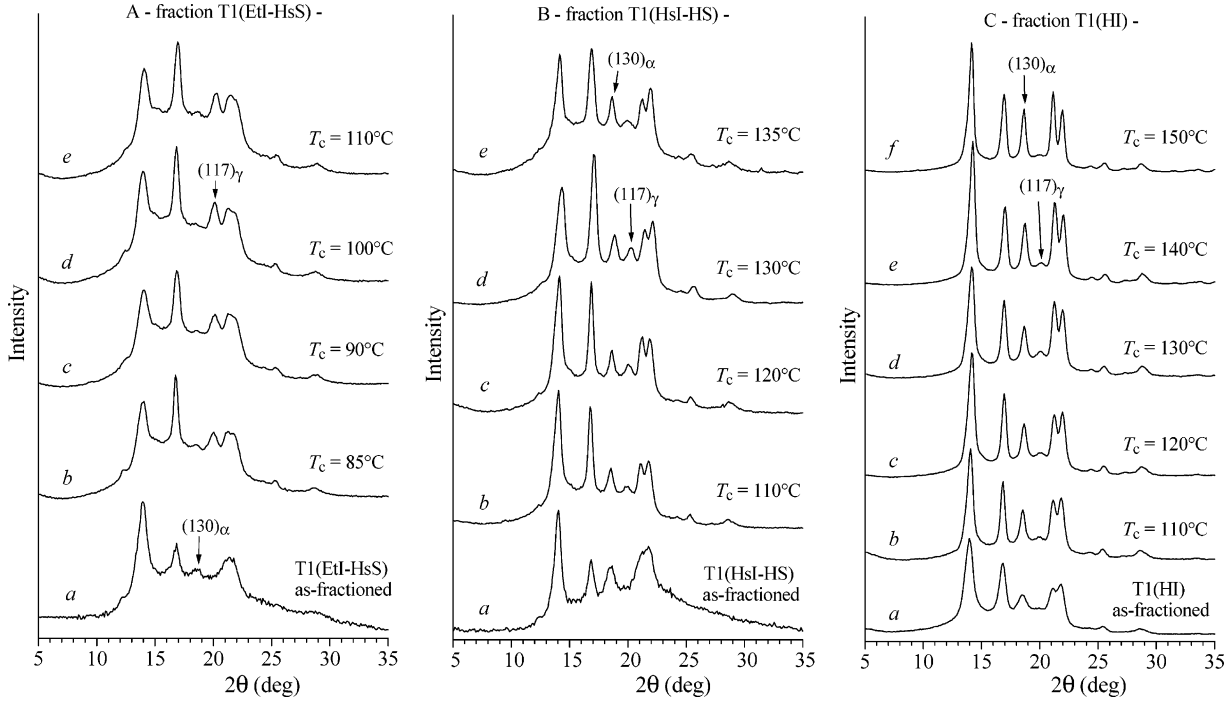

Figure 6. X-ray powder diffraction profiles of samples of the fractions T1(EtI−HsS) (A), T1(HsI−HS) (B), and T1(HI) (C) isothermally crystallized from the melt at the indicated temperatures. The $(130)_\alpha$ reflection of the α form at $2\theta = 18.6°$ and the $(117)_\gamma$ reflection of the γ form at $2\theta = 20.1°$ are indicated.

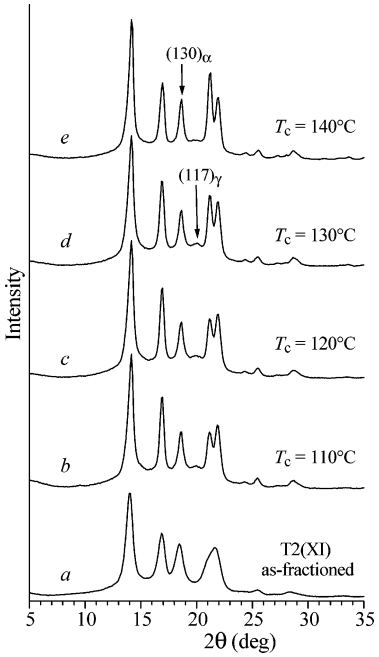

Figure 7. X-ray powder diffraction profiles of samples of the fraction T2(XI) isothermally crystallized from the melt at the indicated temperatures. The $(130)_\alpha$ reflection of the α form at $2\theta = 18.6°$ and the $(117)_\gamma$ reflection of the γ form at $2\theta = 20.1°$ are indicated.

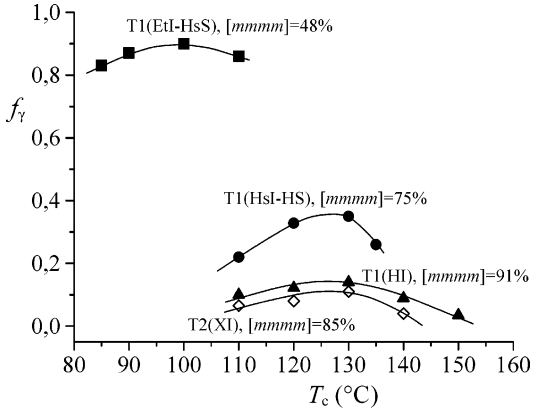

Figure 8. Relative content of γ form of iPP, f_γ, evaluated from the X-ray diffraction profiles, in the samples isothermally crystallized from the melt of the fractions of samples T1 and T2, as a function of the crystallization temperature T_c: (■) fraction T1(EtI−HsS); (●) fraction T1(HsI−HS); (▲) fraction T1(HI); (◇) fraction T2(XI). The stereoregularity of the samples, as concentration of the isotactic pentad *mmmm*, is also indicated.

melt at different temperatures, are reported in Figure 7. It is apparent that the samples crystallize basically in the α form with small amount of γ form, as indicated by the low intensity of the $(117)_\gamma$ reflections at $2\theta = 20.1°$ of the γ form at any crystallization temperature.

For all the fractions of samples T1 and T2, the relative intensity of the $(117)_\gamma$ reflection of the γ form at $2\theta = 20.1°$, with respect to that of the $(130)_\alpha$ reflection of the α form at $2\theta = 18.6°$, increases with increasing the crystallization temperature, reaches a maximum value, and then decreases for a further increase of the crystallization temperature.

The relative amount of the γ form with respect to the α form, f_γ, for the various samples is reported in Figure 8 as a function of the crystallization temperature. The content of the γ form increases with increasing crystallization temperatures, and a maximum amount of the γ form is obtained at temperatures in the range 120−130 °C for the more crystalline fractions T1(HsI−HS), T1(HI), and T2(XI) and at 100 °C for the less crystalline fraction T1(EtI−HsS).

The analysis of the microstructures of the fractions of the iPP samples, performed by ^{13}C NMR (Figures 1 and 2 and Tables 4 and 5), has shown that the iPP chains of the more stereoregular fraction T1(HI) present a small concentration of defects of stereoregularity

mainly represented by isolated *rr* triads. In the ^{13}C NMR spectrum of Figure 1D, besides the resonance of the isotactic pentad *mmmm*, the three signals relative to the pentad stereosequences *mmmr*, *mmrr*, and *mrrm* with intensity ratios close to 2:2:1 (Table 4) are basically present, according to a site control of the propagation mechanism.[30] In the case of the crystalline fraction of the sample T2 (T2(XI)), besides the three signals relative to the pentads *mmmr*, *mmrr*, and *mrrm*, also the signal corresponding to syndiotactic sequences (*rrrr* pentad) is clearly observed (Figure 2B and Table 5).

The chains of the less stereoregular fractions T1(EtI−HsS) and T1(HsI−HS) present *rr* defects, the concentrations of the *mrrm* pentad being 5.6 and 2.2%, respectively (Figure 1B,C and Table 4), but also rather long syndiotactic sequences, as indicated by the presence in the spectra of Figure 1B,C of resonances at 20.8−20.9 ppm, corresponding basically to the *rmrr* pentad and at 20.3 ppm corresponding to *rrrr* sequences. The concentration of the fully syndiotactic *rrrr* pentad is quite high, 9.22% and 4.63% for the chains of the fractions T1(EtI−HsS) and T1(HsI−HS), respectively (Figure 1, Table 4). This indicates that, especially in the chains of the less regular fraction T1(EtI−HsS), quite long syndiotactic sequences are present. The presence of the very weak diffraction peak at $2\theta = 12°$ in the X-ray powder diffraction profiles of the fraction T1(EtI−HsS) of Figures 3c and 6A (profile a) and of samples of the fraction T1(EtI−HsS) crystallized from the melt (profiles b−e of Figure 6A) indicates that the syndiotactic sequences are long enough to crystallize. The reflection at $2\theta = 12°$ corresponds, indeed, to the 200 reflection arising from the crystals of syndiotactic polypropylene in the stable polymorphic form with chains in 2-fold helical conformation.[44] In the case of the more isotactic fraction T1(HsI−HS), with lower concentration of the *rrrr* pentad (4.6%), the intensity of the corresponding reflection at $2\theta = 12°$ in the diffraction profiles of Figure 6B is negligible, indicating the presence of a negligible amount of crystals of syndiotactic polypropylene.

The presence of syndiotactic *rrrr* sequences in some fractions of Ziegler−Natta iPP has been observed and extensively discussed in the literature.[33−38] Moreover, the segregation of most of propagation errors, including syndiotactic sequences, in portions of chains producing stereoblocks has been suggested in various papers.[33−38] However, the possibility that syndiotactic sequences may be present, at least in part, in different macromolecules difficult to separate with the standard methods of extraction with boiling solvents cannot be excluded.[45]

The results of the structural analysis of Figure 8 indicate that for these complex microstructures of Ziegler−Natta iPP samples the amount of γ form, which may develop by melt-crystallizations, increases with increasing the concentration of defects. The maximum amounts of γ form, f_γ(max), evaluated from the maxima of the curves of Figure 8, are nearly 10−15% for the fractions T1(HI) and T2(XI), 35% for the fraction T1-(HsI−HS), and 90% for the fraction T1(EtI−HsS). This result is in agreement with the hypothesis reported in the literature that the γ form crystallizes in samples or fractions of iPP characterized by chains having short regular isotactic sequences.[16,17,19,25−27]

The presence of maxima in the curves of the content of γ form as a function of the crystallization temperature (Figure 8) may be explained as a result of two competing kinetic and thermodynamic effects, as discussed in ref 26 in the case of metallocene-made iPP samples. For samples of iPP containing an appreciable amount of stereodefects, the formation of the γ form is favored because the defects and the α/γ structural disorder are highly tolerated in the γ form. As a consequence, a high amount of γ form develops in the slow crystallizations at high crystallization temperatures. At lower crystallization temperatures the fast crystallization of the α form is instead kinetically favored, giving a low amount of γ form.[26] With increasing crystallization temperature the amount of γ form increases, but at very high crystallization temperatures the crystallization of the defective γ form is too slow because of its lower melting temperature,[26] and the more perfect α form becomes again kinetically favored, so that the amount of γ form decreases (Figure 8).

It is worth noting that the amount of γ form crystallized in the fractions of our Ziegler−Natta iPP samples is much higher (the fraction T1(EtI−HsS) crystallizes almost totally in the γ form, f_γ(max) being 90%) than that found in a recent study by Alamo et al.[39] or in previous works on highly stereoregular iPP fractions.[46−48] In the ref 39 it was reported that the analyzed Ziegler−Natta iPP fractions develop a very low amount of γ form, and it was concluded that the lack of formation of any significant content of the γ form, even in the most defected fraction, is consistent with a nonrandom, blocky intramolecular distribution of defects. The fact that in our sample the two more defected fractions T1(HsI−HS) and T1(EtI−HsS) develop a much higher content of γ form, and the latter crystallizes almost totally in the γ form, indicates that a higher concentration of defects is present in our fractions. This also indicates that different microstructures of chains in Ziegler−Natta iPP can be obtained depending on the catalyst, in particular on the Lewis bases added to the catalyst/cocatalyst system as internal or external donors.

Comparison with Metallocene iPP. The crystallization properties of Ziegler−Natta iPP have been compared with the polymorphic behavior of samples of iPP prepared with metallocene catalysts.[26] The amounts of γ form obtained by melt-crystallization of iPP samples, prepared with the single-center metallocene catalyst *rac*-isopropyliden[bis(3-trimethylsilyl)(indenyl)]$ZrCl_2$ (samples R1, R2, and R3), taken from refs 25 and 26, are compared in Figure 9 with the data obtained for the Ziegler−Natta iPP. As described by Resconi et al.,[28] this metallocene catalyst produces iPP samples characterized by chains containing only defects of stereoregularity (mainly isolated *rr* triads), whose amount depends on the polymerization temperature. The distribution of defects along the chains is random, and no defects of regioregularity are present. This catalyst may be, therefore, taken as a reference catalyst for the single-center metallocene catalysts because it produces very simple chain microstructure, providing the first example of metallocene-made iPP not including regioerrors.[28] These samples are, therefore, the best candidate for comparing the polymorphic behavior with that of our Ziegler−Natta iPP samples not containing regioerrors.

As discussed in refs 25 and 26, for the metallocene iPP samples the content of γ form increases with increasing crystallization temperature, with a maximum at temperatures of 120−130 °C, and increases with increasing concentration of defects of stereoregularity. These data have indicated that the crystallization

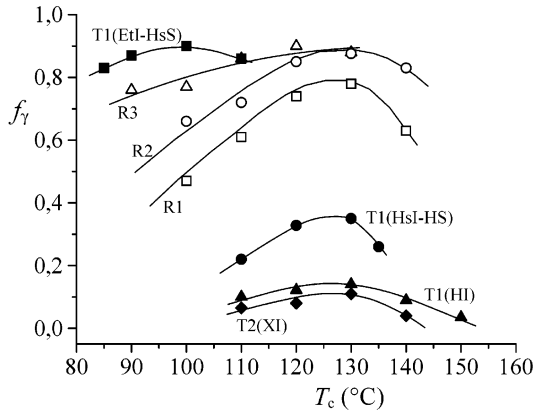

Figure 9. Comparison between the relative contents of γ form of iPP, f_γ, as a function of the crystallization temperature T_c for metallocene-made iPP samples R*i* (taken from refs 25 and 26) and Ziegler−Natta samples T1 and T2, isothermally crystallized from the melt: (■) fraction T1(EtI−HsS), [*mmmm*] = 47.5%; (●) fraction T1(HsI−HS), [*mmmm*] = 74.7%; (▲) fraction T1(HI), [*mmmm*] = 91.4%; (◆) fraction T2(XI), [*mmmm*] = 84.9%; (□) sample R1, [*mmmm*] = 89.0%; (○) sample R2, [*mmmm*] = 87.4%; (△) sample R3, [*mmmm*] = 83.4%.

of the γ form is favored in iPP samples characterized by short regular isotactic sequences.[25,26] The lower the degree of isotacticity, the higher the maximum amount of the crystallized γ form (f_γ(max)) evaluated from the maxima of the curves of Figure 9. In particular, f_γ(max) $\approx$ 78% for the sample R1 ([*mmmm*] = 89.0%) and 90% for the less stereoregular samples R2 and R3 ([*mmmm*] = 87.4 and 83.4%, respectively).[25,26]

The relative stability of α and γ forms of iPP is related to the average length of the fully isotactic sequences comprised between two successive interruptions, and the γ form crystallizes more easily when the regular isotactic sequences are short.[19,25,26] The number of interruptions depends, in turn, on the content of defects and the degree of segregation of the defects along the polymer chain. Since the samples R*i* have a random distribution of configurational errors (mainly isolated *rr* triads), the average length of the fully isotactic sequences, $\langle L_{iso}\rangle$, is inversely proportional to the content of errors ($\langle L_{iso}\rangle = 1/[rr]$). As a consequence, the amount of γ form at a given crystallization temperature turns out to be higher for the less stereoregular sample R3 (with $\langle L_{iso}\rangle$ = 29 monomeric units) than for the samples R2 ($\langle L_{iso}\rangle$ = 38 monomeric units) and R1 ($\langle L_{iso}\rangle$ = 43 monomeric units).[25,26]

As discussed in the previous section, the fractions of the Ziegler−Natta iPP samples T1 and T2 show a similar behavior, with a notable difference in the maximum amount of the crystallized γ form. It is apparent from the comparison of Figure 9 that the more stereoregular fractions T1(HI) and T2(XI) present a content of γ form much lower than that obtained in the sample R1, having a similar isotacticity, at any crystallization temperature. The sample R1, having [*mmmm*] = 89% (Table 3), develops a maximum amount of γ form f_γ(max) = 78% (Figure 9), against the values of only 15% observed for the fraction T(HI), having [*mmmm*] = 91.4%, and 10% for the fraction T2(XI), having [*mmmm*] = 84.9% (Tables 4 and 5).

In the hypothesis that the γ form preferably crystallizes when the regular isotactic sequences are relatively short,[19,25,26] these data indicate that the chains in the samples T1(HI) and T2(XI) present regular isotactic sequences much longer than those of the chains of the sample R1, even though the overall concentration of defects is not very different. In particular, both samples R1 and T1(HI) contain basically only isolated *rr* triad defects ([*rr*] = 2.3% for the sample R1, [*mrrm*] = 1.18% for the fraction T1(HI)), whereas the fraction T2(XI) contains longer syndiotactic sequences ([*rrrr*] = 1.30%, Table 5) along with isolated *rr* triads ([*mrrm*] = 2.08%). It is apparent that the fraction T2(XI) and the sample R1 present nearly the same concentration of the isotactic *mmmm* pentad ([*mmmm*] = 84.9 and 89%, respectively), hence a similar overall stereregularity, but the fraction T2(XI) contains a higher amount of defects. Notwithstanding, the chains of the fraction T2(XI) present regular isotactic sequences much longer than those of the chains of the sample R1.

This result can be explained considering that the chains of Ziegler−Natta and metallocene iPP samples present a different distribution of defects. In the metallocene-made iPP samples R*i* the distribution of defects of stereoregularity along the macromolecular chains is random so that even a small concentration of defects produces frequent interruptions of the isotactic propagation and the regular isotactic sequences turn out to be relatively short even for samples with quite high stereoregularity.[26] This explains the high concentration of γ form (78−90%) obtained in the relatively high isotactic samples R1, R2, and R3 (Figure 9).

In the sample T1(HI) and T2(XI) the same amount of stereodefects is not randomly distributed along the chains; the defects are segregated in more irregular, noncrystallizable portions of chains so that the more regular isotactic sequences are always very long and crystallize preferably in the α form.

A rough evaluation of the average length of the isotactic sequences in polypropylene chains may be obtained with the empirical method proposed by us in ref 25 for stereoblock polypropylene. The method is based on the use of a calibration plot of the maximum amount of the γ form, f_γ(max), as a function of the average length of the fully isotactic sequences $\langle L_{iso}\rangle$ obtained for iPP samples prepared with metallocene catalysts having a random distribution of defects. The average length of the fully isotactic sequences may be evaluated as $\langle L_{iso}\rangle = 1/\epsilon$, with ϵ the total concentration of errors determined by the ^{13}C NMR analysis. For these samples the maximum amount of γ form, which can be obtained by the melt-crystallization procedures, is roughly linear with the logarithm of $\langle L_{iso}\rangle$ (see Figure 7 of ref 25). If this linear relationship is kept general whatever the distribution of defects, it is possible to find the length of the fully isotactic sequences also for polypropylene samples characterized by nonrandom distribution of defects from the values of f_γ(max). The calibration plot of f_γ(max) as a function of $\langle L_{iso}\rangle$ is reported in Figure 10, and the indirect method is applied to the various fractions of the Ziegler−Natta iPP. From the values of f_γ(max) = 10% and 15%, evaluated from Figure 9 for the fractions T2(XI) and T1(HI), respectively, values of the average length of the isotactic sequences $\langle L_{iso}\rangle$ of 250 and 220 monomeric units for the chains of the fractions T2(XI) and T1(HI), respectively, have been found (Figure 10).

The content of γ form is higher in the case of the more irregular fractions of the Ziegler−Natta iPP sample, T1(HsI−HS) and T1(EtI−HsS) (Figure 9). It is apparent, however, that even though the fraction T1(HsI−HS) is less stereoregular ([*mmmm*] = 75%, Table 4) than the

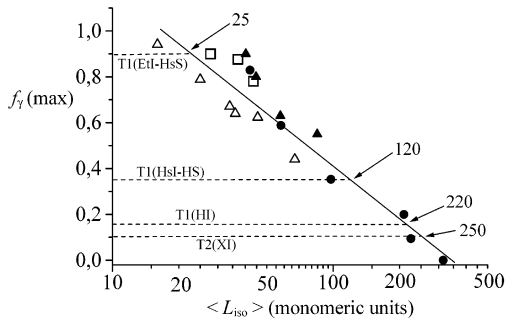

Figure 10. Maximum amount of γ form of iPP obtained upon melt-crystallization procedures for various samples of iPP, f_γ(max), as a function of the average length of fully isotactic sequences, $\langle L_{iso}\rangle$, comprised between two consecutive interruptions (defects): (□) samples R*i* from refs 25 and 26; (△) data from ref 22; (●) data from ref 19; (▲) data from ref 23. The values of f_γ(max) evaluated from Figure 9 for the fractions of Ziegler−Natta iPP samples T1(EtI−HsS), T1(HsI−HS), T1(HI), and T2(XI) are also shown as horizontal dashed lines. The intercepts of these dashed lines on the straight line give the average lengths of fully isotactic sequences $\langle L_{iso}\rangle$ for the fractions of the T1 and T2 samples.

metallocene samples R*i*, it shows a maximum amount of γ form of 35%, much lower than those observed for the samples R*i*. As discussed above, the fraction T1(HsI−HS) is characterized by a appreciable concentration of *rr* defects (2.2%, Table 4) and a high concentration of syndiotactic sequences ([*rrrr*] = 4.6%, Table 4). Despite this high concentration of defects, the sample T1(HsI−HS) still crystallizes preferably in the α form, f_γ(max) being only 35% (Figure 9). This indicates that also for this fraction the regular isotactic sequences are still quite long, even in the presence of so many defects, in any case longer than those in the chains of R*i* samples, which instead are characterized by a lower concentration of defects. This suggests that also for the fraction T1(HsI−HS) the defects (*rr* stereodefects and longer syndiotactic sequences *rrrr*) are segregated in more irregular noncrystallizable (or hardly crystallizable) portions of the chains. The more regular isotactic sequences would be, therefore, rather long and able to crystallize preferably in the α form, and the amount of the γ form turns out to be low even though the overall degree of stereoregularity, as evaluated by the ^{13}C NMR spectrum, is very low.

From Figure 10, by using the structural datum of the maximum amount of γ form of 35%, an average length of the isotactic sequences $\langle L_{iso}\rangle$ of 120 monomeric unit has been evaluated for the chains of the fraction T1(HsI−HS). In this fraction the iPP chains are characterized by a microstructure consisting in long, rather regular, isotactic sequences linked to more irregular sequences. The latter contains the major part of stereodefects mainly consisting in *rr* triads and longer ...*rrrr*... syndiotatic sequences. The hypothesis of a stereoblock microstructure is in agreement with the experimental observation that the fraction T1(HsI−HS) presents a melting temperature of 148 °C (Table 1), higher than that of the more stereoregular sample R1 (144 °C, Table 3).

The presence in the fraction T1(HsI−HS) of a high concentration of the syndiotactic pentad ([*rrrr*] = 4.6%, Table 4) indicates that in this stereoblock microstructure the more irregular sequences contain relatively long syndiotactic sequences along with atactic sequences. This explains the presence of the weak reflection at $2\theta = 12°$ in the diffraction profiles of Figure 6B, which indicates the presence of crystals of syndiotactic polypropylene (sPP),[44] arising from the syndiotactic sequences long enough to crystallize. However, the possibility that the syndiotactic sequences are more concentrated in different macromolecules, difficult to separate with the methods of the extraction with boiling solvent, cannot be excluded.

Figures 8 and 9 show that the more irregular fraction T1(EtI−HsS) of the Ziegler−Natta iPP sample crystallizes almost totally in the γ form, the maximum amount of γ form, f_γ(max), being nearly 90%, similar to that obtained for the samples R2 and R3. It is worth noting, however, that the metallocene iPP samples R2 and R3, having [*mmmm*] = 87.4% and 83.4%, respectively (Table 3), are much more stereoregular than the fraction T1(EtI−HsS) of the Ziegler−Natta sample, which is characterized by [*mmmm*] = 48% (Table 4). This clearly indicates that samples or fractions of Ziegler−Natta iPP may crystallize from the melt at atmospheric pressure almost totally in the γ form only when the concentration of defects is much higher than that needed for the metallocene-made iPP samples. In fact, the samples R2 and R3 contain only 2.6 and 3.4% of randomly distributed *rr* defects (Table 3), sufficient to make the regular isotactic sequences very short ($\langle L_{iso}\rangle$ = 30−40 monomeric units), inducing crystallization almost totally in the γ form (Figure 9). The fraction T1(EtI−HsS) is characterized by chains containing a high concentration of defects, consisting in isolated *rr* triads (5.6%), isolated *r* diads, and long syndiotactic sequences ([*rrrr*] = 9.2%, Table 4). Only with a so high concentration of defects, sufficiently short isotactic sequences are obtained so that an almost total crystallization in the γ form is induced. From the value of f_γ(max) = 90% and from Figure 10, an average length of the isotactic sequences $\langle L_{iso}\rangle$ of 25 monomeric units has been evaluated for the chains of the fraction T1(EtI−HsS), similar to that of the sample R3 (Table 3).

This result indicates that very different amounts of defects produce similar average lengths of the isotactic sequences in the samples R3 and T1(EtI−HsS) and suggests that also for the fraction T1(EtI−HsS) most of the defects (*rr* triads and longer ...*rrrr*... syndiotatic sequences) are segregated in more irregular noncrystallizable portions of the chains, producing slightly more regular isotactic sequences able to crystallize. These sequences are, however, poorly isotactic, contain an appreciable amount of defects, and tend to crystallize in the γ form (Figure 6A). This microstructure is in agreement with the experimental observation that the fraction T1(EtI−HsS) crystallizes either from solution (Figure 3c) or from the melt (Figure 6A) with a relatively high crystallinity (nearly 17%) and melting temperature (114 °C, Table 1), despite the high content of defects.

The presence in the fraction T1(EtI−HsS) of syndiotactic sequences ([*rrrr*] = 9.2%, Table 4) indicates that the more irregular sequences contain relatively long syndiotactic sequences, able to crystallize, along with atactic sequences. The syndiotactic sequences are long enough to crystallize, and this explains the presence of the weak reflection at $2\theta = 12°$ in the diffraction profiles of Figure 6A, which indicates the presence of crystals of sPP.[44]

As shown in Table 5, higher concentrations of syndiotactic sequences have been found in the more irregular, nearly amorphous, xylene soluble fraction of the

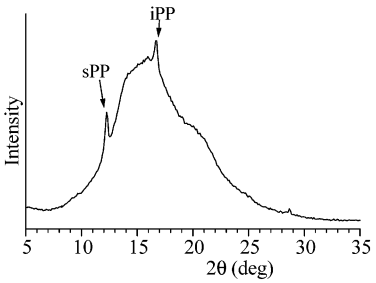

Figure 11. X-ray powder diffraction profile of the fraction T2-(AI−XS) of the iPP sample T2 crystallized by slow cooling the melt to room temperature. Reflections typical of crystals of iPP and sPP are indicated.

sample T2 (fraction T2(AI-XS)). In this sample the concentrations of the fully isotactic and syndiotactic pentads are basically the same ([*mmmm*] = 17.73% and [*rrrr*] = 16.96%, Table 5). As already shown in Figure 5, this sample is basically amorphous, but the short isotactic and syndiotactic sequences are able to crystallize, as indicated by the presence of the weak diffraction peaks at $2\theta = 17°$, arising from crystals of iPP and at $2\theta = 12°$, arising from crystals of sPP. The X-ray powder diffraction profile of the fraction T2(AI−XS) crystallized from the melt, by slowly cooling the melt to room temperature, is reported in Figure 11. It is apparent that both the crystallinities from iPP and sPP are slightly improved, as indicated by the increase of the intensities of both reflections at $2\theta = 12°$ and 17° (compare Figures 5b and 11). As discussed above, for these irregular fractions the small level of iPP crystallinity (5−10%), arising from the poorly isotactic sequences, produces diffraction profiles characterized by the presence of only the diffraction peak at $2\theta = 17°$ (Figures 3b, 5b, and 11), corresponding to the $(040)_\alpha$ or $(008)_\gamma$ reflections of the α and γ forms, respectively. This indicates that the crystals of iPP are in disordered α/γ modifications intermediate between the α and γ forms.[24,26] These disordered modifications of the γ form have been described to explain the X-ray powder and fiber diffraction patterns of poorly isotactic polypropylene prepared with metallocene catalysts.[24] This kind of disorder is also present in the crystals of the γ form crystallized from much higher isotactic samples, prepared with different metallocene catalysts.[26] The data reported in this paper, in particular the diffraction profiles of Figures 3b, 5b, and 11, and the low intensities of the $(130)_\alpha$ and $(117)_\gamma$ reflections at $2\theta = 18.6°$ and 20.1°, respectively, in the diffraction profiles of Figures 3a,c,e and 5a, allow to recognize for the first time that also Ziegler−Natta iPP samples crystallize in these disordered modifications of the γ form.

It is worth noting that evidences of a nonuniform distribution of defects in chains of fractions of Ziegler−Natta iPP have recently been provided by Alamo and Randall et al.[39,40] by using indirect methods of the analysis of the crystallization properties, together with traditional method of the NMR analysis. In these studies the analysis of the linear spherulitic growth rates, the polymorphic behavior, and the pentad/heptad distributions from ^{13}C NMR have indicate that Ziegler−Natta iPP samples contain a fraction characterized by chains having a stereoblock microstructure with isotactic sequences length of 5−25 monomeric units, a fraction with longer isotactic sequences (around 200 monomeric units), and a highly isotactic fraction characterized by chains with much longer isotactic sequences.[39,40] These results are consistent with the three-state statistical models generally used to describe the NMR data.[35] Our results are in agreement with these studies.

Nonisothermal Melt-Crystallization. The crystallization from the melt of the Ziegler−Natta iPP samples T1 and T2 has also been studied in nonisothermal conditions. The X-ray diffraction profiles of the fractions T1(EtI−HsS), T1(HsI−HS), and T1(HI) of the sample T1 crystallized by cooling the melt at cooling rates of 1, 2.5, 10, 20, and 40 °C/min are reported in Figure 12. Similar diffraction profiles for the fraction T2(XI) are reported in Figure 13. Also in this case the samples crystallize in mixtures of α and γ forms. It is apparent that for all samples the crystallization of the α form is

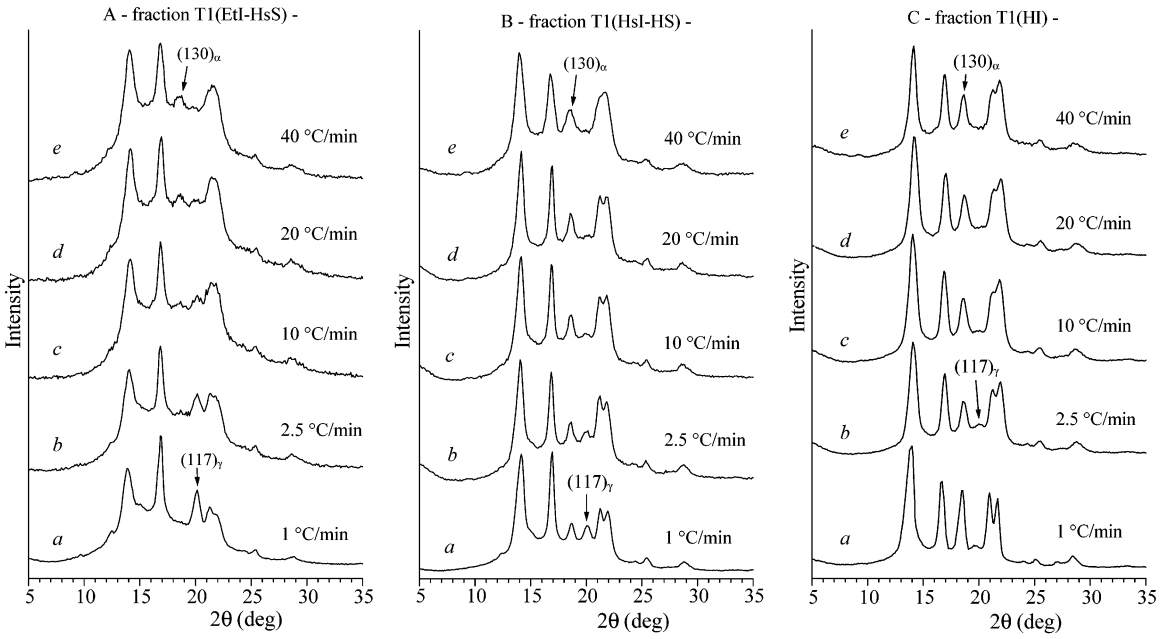

Figure 12. X-ray powder diffraction profiles of samples of the fractions T1(EtI−HsS) (A), T1(HsI−HS) (B), and T1(HI) (C) of the iPP sample T1 crystallized by cooling the melt to room temperature at the indicated cooling rates. The $(130)_\alpha$ reflection of the α form at $2\theta = 18.6°$ and the $(117)_\gamma$ reflection of the γ form at $2\theta = 20.1°$ are indicated.

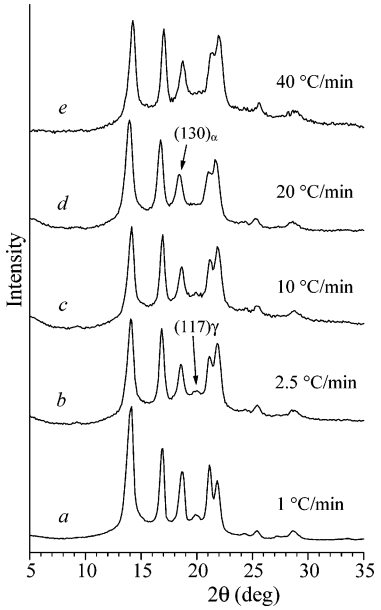

Figure 13. X-ray powder diffraction profiles of samples of the fraction T2(XI) of the iPP sample T2 crystallized by cooling the melt to room temperature at the indicated cooling rates. The $(130)_\alpha$ reflection of the α form at $2\theta = 18.6°$ and the $(117)_\gamma$ reflections of the γ form at $2\theta = 20.1°$ are indicated.

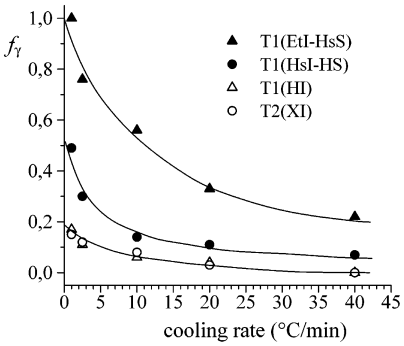

Figure 14. Relative content of γ form of iPP, f_γ, evaluated from the X-ray diffraction profiles of Figures 12 and 13, in the samples crystallized from the melt of fractions of samples T1 and T2, as a function of the cooling rate: (▲) fraction T1(EtI−HsS); (●) fraction T1(HsI−HS); (△) fraction T1(HI); (○) fraction T2(XI).

favored by fast cooling rates, whereas slow cooling rates induce the crystallization of the γ form. The content of γ form is very high for the irregular fraction T1(EtI−HsS) crystallized at very low cooling rate (profile a in Figure 12A). At high cooling rates this fraction crystallizes instead in α/γ disordered modifications, as indicated by the very low intensities of both $(130)_\alpha$ and $(117)_\gamma$ reflections at $2\theta = 18.6°$ and 20.1°, respectively, in the X-ray diffraction profile e of Figure 12A. The more stereoregular fractions T1(HI) and T2(XI) crystallize basically in the α form with very low γ form content at any cooling rates (Figures 12C and 13). The content of γ form, evaluated from the X-ray diffraction profiles of Figures 12 and 13, is reported in Figure 14 as a function of the cooling rate. The extrapolation to zero cooling rate of the values of f_γ gives the maximum amounts of γ form, f_γ(max), which can be obtained for each sample in these conditions. These values are only slightly higher than the maximum amount of γ form obtained by isothermal crystallization from the melt, deduced from the maxima of the curves of Figure 8.

These data clearly indicate that, as already shown for metallocene-made iPP,[26] the crystallization of α and γ forms of iPP depends on thermodynamic and kinetic factors. The α form is always kinetically favored over the γ form; even in the case of samples or fractions of iPP characterized by chains with relatively short regular isotactic sequences (fraction T1(EtI−HsS)), which crystallize almost totally in the γ form when slowly crystallized from the melt at high temperatures (Figure 6A) or by slow cooling the melt to room temperature (profiles a and b in Figure 12A), the α form is obtained when the crystallization is very fast by quenching the melt to room temperature (profile e in Figure 12A).

Conclusions

The polymorphic behavior of iPP samples prepared with heterogeneous Ziegler−Natta catalysts has been analyzed and compared with the behavior of iPP samples prepared with a single-center homogeneous metallocene catalyst.

As described in the literature, the crystallization properties of metallocene-made iPP depends on the kind, amount, and distribution of defects (stereo- and regiodefects) in the macromolecular iPP chains.[25,26] Mixtures of the α and γ forms are generally obtained by crystallization from the melt, and the relative content of γ form increases with increasing the content of defects. The crystallization of the γ form is favored in samples characterized by chains with short regular isotactic sequences. In chains of iPP samples prepared with metallocene catalysts the distribution of defects is random, and the length of fully isotactic sequences is roughly inversely related to the content of insertion errors.[25,26] As a consequence, even a small amount of defects reduces the length of the regular isotactic sequences, inducing crystallization of the γ form.[19,25,26]

Different samples of Ziegler−Natta iPP samples, prepared with $MgCl_2$-supported catalysts modified by adding different Lewis bases as internal or external donors, have been fractionated by extraction with boiling solvents. The various fractions have been crystallized from the melt and the polymorphic behavior analyzed by X-ray diffraction. Appreciable amounts of γ form crystallize in more stereoirregular fractions. In particular, the fraction insoluble in diethyl ether and soluble in hexane (T1(EtI−HsS)) crystallizes from the melt almost totally in the γ form. The more stereoregular fractions, insoluble in *n*-heptane or *o*-xylene (T1(HI) and T2(XI)), crystallize basically in the α form. This confirms that, even in the case of Ziegler−Natta iPP samples, which, as generally accepted, crystallize in the stable α form,[1−4,10−14,39,46−48] the γ form may develop by melt-crystallization at atmospheric pressure in fractions containing high concentration of defects.

The relative amount of γ form crystallized from the melt is, however, much lower that that observed in samples of metallocene-made iPP containing comparable amount of defects. This indicates that in Ziegler−Natta iPP samples the regular isotactic sequences are longer than those present in chains of metallocene-made iPP samples having a similar overall concentration of defects.

The different polymorphic behavior of metallocene and Ziegler−Natta iPP samples is related to the different distribution of defects in the chains generated by the different kinds of catalytic systems. The distribution of defects, indeed, influences the average length of the

crystallizable (fully isotactic) sequences. While in the metallocene iPP the defects are randomly distributed along the chains, in Ziegler−Natta iPP samples the majority of the defects are segregated in a small fraction of poorly crystallizable macromolecules or in more irregular portions of the chain, so that much longer fully isotactic sequences can be produced, leading to the crystallization of the α form even for a relatively high overall concentration of defects.

These results confirm the idea suggested by us in ref 25 that the structural analysis of iPP, in particular the crystallization of the γ form, may give information about the microstructure of the polymer chains and may be used as a practical tool to test the degree of segregation of defects, revealing the presence of stereoblocks.[25] As proposed by us in ref 25, the measure of the maximum amount of γ form crystallized from the melt may be used as an indirect method to evaluate the average length of isotactic sequences.

The more stereoregular fractions T1(HI) and T2(XI) present a content of γ form much lower than that obtained in the metallocene iPP sample R1, having a similar overall concentration of defects, consisting mainly in isolated *rr* triads. In the sample T1(HI) and T2(XI) the same amount of stereodefects is segregated in more irregular, noncrystallizable, portions of chains so that the more regular isotactic sequences are always very long and crystallize preferably in the α form. Values of the average length of the isotactic sequences $\langle L_{iso} \rangle$ of 250 and 220 monomeric units for the chains of the fractions T2(XI) and T1(HI), respectively, have been estimated.

The content of the γ form is higher in the case of the more irregular fractions of the Ziegler−Natta iPP sample, T1(HsI−HS) and T1(EtI−HsS). However, even though the fraction T1(HsI−HS) is less stereoregular ([*mmmm*] = 75%) than the metallocene samples R*i*, it shows a maximum amount of γ form much lower than those observed for the samples R*i*. This suggests that also for the fraction T1(HsI−HS) the defects (isolated *rr* triads and *r* diads and longer syndiotactic sequences *rrrr*) are segregated in more irregular noncrystallizable (or hardly crystallizable) portions of the chains. The more regular isotactic sequences would be, therefore, rather long and able to crystallize preferably in the α form. An average length of the isotactic sequences $\langle L_{iso} \rangle$ of 120 monomeric units has been evaluated for the chains of the fraction T1(HsI−HS).

The presence in the fraction T1(HsI−HS) of a high concentration of the syndiotactic pentad indicates that, in this stereoblock microstructure, the more irregular sequences contain relatively long syndiotactic sequences (able to crystallize producing a very small amount of crystals of syndiotactic polypropylene) along with atactic sequences. However, the possibility that the syndiotactic sequences are more concentrated in different macromolecules, difficult to separate with the methods of the extraction with boiling solvent, cannot be excluded.

The more irregular fraction T1(EtI−HsS) of the Ziegler−Natta iPP sample crystallizes almost totally in the γ form, as in the case of the more stereoregular samples R2 and R3. This clearly indicates that samples or fractions of Ziegler−Natta iPP may crystallize from the melt almost totally in the γ form only when the concentration of defects is much higher than that needed for the metallocene-made iPP samples. In fact, the samples R2 and R3 contain only 2.6 and 3.4% of randomly distributed *rr* defects (Table 3), sufficient to make the regular isotactic sequences very short ($\langle L_{iso} \rangle$ = 30−40 monomeric units), inducing crystallization almost totally in the γ form. The fraction T1(EtI−HsS) is characterized by chains containing a much higher concentration of defects, consisting in isolated *rr* triads, *r* diads, and long syndiotactic sequences. Only with a so high concentration of defects, sufficiently short isotactic sequences are obtained so that an almost total crystallization in the γ form is induced. An average length of the isotactic sequences $\langle L_{iso} \rangle$ of 25 monomeric units has been evaluated for the chains of the fraction T1(EtI−HsS), similar to that of the sample R3. Also for the fraction T1(EtI−HsS), most of the defects are segregated in more irregular noncrystallizable portions of the chains, producing slightly more regular isotactic sequences able to crystallize. The latter contain, however, an appreciable amount of defects inducing crystallization of the γ form. The low melting temperature of 114 °C of the as-fractioned sample T1(EtI−HsS), compared to that of the sample R3 (137 °C), may probably be due to the presence of appreciable amount of defects in the crystalline domains and to the broader distribution of lengths of crystallizable isotactic sequences in the fractions of Ziegler−Natta iPP.

Acknowledgment. Financial support from Basell Polyolefins (Ferrara, Italy) and from the "Ministero dell'Istruzione, Università e Ricerca Scientifica" (PRIN 2002 and Cluster C26 projects) is gratefully acknowledged. We thank Dr. Luigi Resconi of Basell Polyolefins, Ferrara, for providing the meltallocene-made iPP samples and Dr. Ofelia Fusco of Basell for providing the Ziegler−Natta iPP samples. The NMR polymer characterizations were carried out at Centro di Metodologie Chimico-Fisiche, University of Naples Federico II.

References and Notes

(1) Natta, G.; Corradini, P. *Nuovo Cimento Suppl.* **1960**, *15*, 40.
(2) Brückner, S. Meille, S. V.; Petraccone, V.; Pirozzi, B. *Prog. Polym. Sci.* **1991**, *16*, 361.
(3) Mencik, Z. *J. Macromol. Sci., Phys.* **1972**, *6*, 101.
(4) Hikosaka, M.; Seto, T. *Polym. J.* **1973,** *5*, 111.
(5) Meille, S. V.; Ferro, D. R.; Bruckner, S.; Lovinger, A.; Padden, F. J. *Macromolecules* **1994**, *27*, 2615.
(6) Dorset, D. L.; McCourt, M. P.; Kopp, S.; Schumacher, M.; Okihara, T.; Lotz, B. *Polymer* **1998**, *39*, 6331. Stocker, W.; Schumaker, M.; Graff, S.; Thierry, A.; Wittmann, J.-C.; Lotz, B. *Macromolecules* **1998**, *31*, 807.
(7) Brückner, S.; Meille, S. V. *Nature (London)* **1989**, *340*, 455.
(8) Meille, S. V.; Brückner, S.; Porzio, W. *Macromolecules* **1990**, *23*, 4114.
(9) Corradini, P.; Petraccone, V.; De Rosa, C.; Guerra, G. *Macromolecules* **1986**, *19*, 2699.
(10) Guerra, G.; Petraccone, V.; Corradini, P.; De Rosa, C.; Napolitano, R.; Pirozzi, B.; Giunchi, G. *J. Polym. Sci., Polym. Phys. Ed.* **1984**, *22*, 1029.
(11) De Rosa, C.; Guerra, G.; Napolitano, R.; Petraccone, V.; Pirozzi, B. *Eur. Polym. J.* **1984**, *20*, 937.
(12) De Rosa, C.; Guerra, G.; Napolitano, R.; Petraccone, V.; Pirozzi, B. *J. Therm. Anal.* **1985**, *30*, 1331.
(13) Corradini, P.; Giunchi, G.; Petraccone, V.; Pirozzi, B.; Vidal, H. M. *Gazz. Chim. Ital.* **1980**, *110*, 413.
(14) Auriemma, F.; Ruiz de Ballesteros, O.; De Rosa, C.; Corradini, P. *Macromolecules* **2000**, *33*, 8764.
(15) Kardos, J. L.; Christiansen, W.; Baer, E. *J. Polym. Sci.* **1966**, *A-2*, 777. Pae, K. D.; Morrow, D. R.; Sauer, J. A. *Nature (London)* **1966**, *211*, 514. Pae, K. D. *J. Polym. Sci.*, **1968**, *A-2*, 657. Sauer, J. A.; Pae, K. D. *J. Appl. Phys.* **1968**, *39*, 4959. Morrow, D. R. *J. Macromol. Sci., Phys. Ed.* **1969**, *B3*, 53.
(16) Lotz, B.; Graff, S.; Wittmann, J. C. *J. Polym. Sci., Polym. Phys.* **1986**, *24*, 2017. Kojima, M. *J. Polym. Sci.* **1967**, *5*, 245. Kojima, M. *J. Polym. Sci.* **1968**, *A-2*, 1255. Morrow, D. R.; Newman, B. A. *J. Appl. Phys.* **1968**, *39*, 4944.
(17) Turner-Jones, A. *Polymer* **1971**, *12*, 487.

(18) Resconi, L.; Cavallo, L.; Fait, A.; Piemontesi, F. *Chem. Rev.* **2000**, *100*, 1253.
(19) Alamo, R. G.; Kim, M. H.; Galante, M. J.; Isasi, J. R.; Mandelkern, L. *Macromolecules* **1999**, *32*, 4050.
(20) VanderHart, D. L.; Alamo, R. G.; Nyden, M. R.; Kim, M. H.; Mandelkern, L. *Macromolecules* **2000**, *33*, 6078.
(21) Alamo, R. G.; VanderHart, D. L.; Nyden, M. R.; Mandelkern, L. *Macromolecules* **2000**, *33*, 6094.
(22) Thomann, R.; Wang, C.; Kressler, J.; Mulhaupt, R. *Macromolecules* **1996**, *29*, 8425.
(23) Thomann, R.; Semke, H.; Maier, R. D.; Thomann, Y.; Scherble, J.; Mulhaupt, R.; Kressler, J. *Polymer* **2001**, *42*, 4597.
(24) Auriemma, F.; De Rosa, C.; Boscato, T.; Corradini, P. *Macromolecules* **2001**, *34*, 4815.
(25) De Rosa, C.; Auriemma, F.; Circelli, T.; Waymouth, R. M. *Macromolecules* **2002**, *35*, 3622.
(26) Auriemma, F.; De Rosa, C. *Macromolecules* **2002**, *35*, 9057.
(27) De Rosa, C.; Auriemma, F.; Circelli, T.; Longo, P.; Boccia, A. C. *Macromolecules* **2003**, *36*, 3465.
(28) Resconi, L.; Piemontesi, F.; Camurati, I.; Sudmeijer, O.; Ninfant'ev, I. E.; Ivchenko, K. V.; Kuz'mina, L. *J. Am. Chem. Soc.* **1998**, *120*, 2308.
(29) Coates, G. W.; Waymouth, R. M. *Science* **1995**, *267*, 217.
(30) Zambelli, A.; Locatelli, P.; Bajo, G.; Bovey, F. A. *Macromolecules* **1975**, *8*, 687. Wolfsgruber, C. Zannoni, G.; Rigamonti, E.; Zambelli, A. *Makromol. Chem.* **1975**, *176*, 2765. Pavan, A.; Provasoli, A.; Moraglio, G.; Zambelli, A. *Makromol. Chem.* **1977**, *178*, 1099. Zambelli, A.; Locatelli, P.; Provasoli, A.; Ferro, D. R. *Macromolecules* **1980**, *13*, 267.
(31) Chûjô, R. *Kagaku* **1981**, *36*, 420. Zhu, S. N.; Yang, X. Z.; Chûjô, R. *Polym. J.* **1983**, *12*, 859. Inoue, Y.; Itabashi, Y.; Chûjô, R.; Doi, Y. *Polymer* **1984**, *25*, 1640. Hayashi, T.; Inoue, Y.; Chûjô, R.; Doi, Y. *Polymer* **1989**, *30*, 1714.
(32) Doi, Y. *Makromol. Chem., Rapid Commun.* **1982**, *3*, 635.
(33) Paukkeri, R.; Vaananen, T.; Lehtinen, A. *Polymer* **1993**, *34*, 2488. Paukkeri, R.; Lehtinen, A. *Polymer* **1994**, *35*, 1673. Paukkeri, R.; Iiskola, E.; Lehtinen, A.; Salminen, H. *Polymer* **1994**, *35*, 2636. Lehtinen, A.; Paukkeri, R. *Macromol. Chem. Phys.* **1994**, *195*, 1539.
(34) Chadwick, J. C.; Miedema, A.; Ruisch, B. J.; Sudmeijer, O. *Makromol. Chem.* **1992** *193*, 1463.
(35) Busico, V.; Corradini, P.; De Biasio, R.; Landriani, L.; Segre, A. I. *Macromolecules* **1994**, *27*, 4521. Busico, V.; Cipullo, R.; Corradini, P.; Landriani, L.; Vacatello, M. *Macromolecules* **1995**, *28*, 1887. Busico, V.; Cipullo, R.; Corradini, P.; De Biasio, R. *Macromol. Chem. Phys.* **1995**, *196*, 491. Busico, V.; Cipullo, R.; Talarico, G.; Segre, A. L.; Chadwick, J. C. *Macromolecules* **1997**, *30*, 4786. Busico, V.; Cipullo, R.; Monaco, G.; Vacatello, M.; Segre, A. L. *Macromolecules* **1997**, *30*, 6251. Busico, V.; Cipullo, R.; Monaco, G.; Talarico, G.; Vacatello, M.; Chadwick, J. C.; Segre, A. L.; Sudmeijer, O. *Macromolecules* **1999**, *32*, 4173.
(36) Morini, G.; Albizzati, E.; Balbontin, G.; Mingizzi, I.; Sacchi, M. C.; Forlini, F.; Tritto, I. *Macromolecules* **1996**, *29*, 5770.
(37) Randall, J. C. *Macromolecules* **1997**, *30*, 803.
(38) Viville, P.; Daoust, D.; Jonas, A. M.; Nysten., B.; Legras, R.; Dupire, M.; Michel, J.; Debras, G. *Polymer* **2001**, *42*, 1953.
(39) Alamo, R. G.; Blanco, J. A.; Agarwal, P. K.; Randall, J. C. *Macromolecules* **2003**, *36*, 1559.
(40) Randall, J. C.; Alamo, R. G,; Agarwal, P. K.; Ruff, C. J. *Macromolecules* **2003**, *36*, 1572.
(41) (a) Ram Mohan Rao, M. V.; Yaseen, M. *J. Appl. Polym. Sci.* **1986**, *31*, 2501. (b) Moraglio, G. *Chim. Ind.* **1959**, *9*, 879.
(42) Wunderlich, B. In *Macromolecular Physics;* Academic Press: New York, 1973; Vol. I, p 63.
(43) Turner-Jones, A.; Aizlewood, J. M.; Beckett, D. R. *Makromol. Chem.* **1964**, *75*, 134.
(44) Natta, G. *J. Polym. Sci.* **1959**, *34*, 531. Corradini, P.; Natta, G.; Ganis, P.; Temussi, P. A. *J. Polym. Sci., Part C* **1967**, *16*, 2477. De Rosa, C.; Corradini, P. *Macromolecules* **1993**, *26*, 5711.
(45) Natta, G.; Pasquon, I.; Corradini, P.; Peraldo, M.; Pegoraro, M.; Zambelli, A. *Rend. Fis. Acc. Lincei* **1960**, *28*, 539.
(46) Cheng, S. Z. D.; Janimak, J. J.; Zhang, A.; Hsieh, E. T. *Polymer* **1991**, *32*, 648.
(47) Janimak, J. J.; Cheng, S. Z. D.; Giusti, P. A.; Hsieh, E. T. *Macromolecules* **1991**, *24*, 2253.
(48) Janimak, J. J.; Cheng, S. Z. D.; Zhang, A.; Hsieh, E. T. *Polymer* **1992**, *33*, 728.

MA035295Q